# Scanning force microscopy experiments probing micromechanical properties on polymer surfaces using harmonically modulated friction techniques I. Principles of operation

Heinz Sturm

Department "Performance of Polymer Materials"
Federal Institute for Materials Research and Testing (BAM)
Unter den Eichen 87, D-12205 Berlin, Germany

SUMMARY: Applying a high-frequency lateral vibration between the sample surface and the tip of a scanning force microscope (SFM), a harmonically modulated lateral (friction) force image can be obtained using lock-in techniques. The principles of operation are explained, in particular the dramatic decrease of image artefacts generally caused by topography cross-talk and laser beam interference. Flat interfaces between the two immiscible polymers, poly(methyl methacrylate) (PMMA) and polystyrene (PS), are prepared on a sodium chloride single crystal from the melt. These samples are used to evaluate the appropriate model for the tip-sample interaction geometry. The relationship between frictional and normal force does not follow Amonton's law. This shows that a single-asperity interaction between the tip and sample surface can be considered. Using the new technique, local measurements of shear strength and Young's modulus can be performed.

## Introduction

Since first publications on scanning (atomic) force microscopy (SFM, AFM) in 1986[1)], many attempts have been made to extend the ability of this technique to give local analysis of materials or surface composition contrasts. Thus, measurements of, e.g., mechanical[2)], thermal[3)] and electric[4)] surface properties were evaluated in the past. The investigation of polymers with the so-called SFM force modulation techniques, using vibration in the normal direction to the sample surface to probe modulus and viscosity, sometimes runs into difficulties: abrasion of softer parts and contamination of the vibrating tip by pulled-off polymer chains can occur even with small vibration amplitudes and contact forces. In this work, a technique for measuring harmonically modulated friction is used which, after prognosis of Israelachvilli et al.[5)], should be suitable for investigation of micromechanical surface properties of polymers. An additional advantage of this technique is the reduced dynamic indentation depth of the tip. Compared with procedures modulating the force or displacement in the direction normal to the surface, the resistance of the surface to abrasion should be higher, though it is limited by the surface shear strength.

 CCC 1022-1360/99/$ 17.50+.50/0

In SFM, the lateral force between the tip and sample surface leads to a torsion of the tip-carrying cantilever during the scanning process[6]. This torsion can be measured by using the intensity difference of two corresponding photodiode segments and can be visualised as an image, which can be interpreted as a contrast of local frictional processes (lateral force microscopy, LFM)[7]. But only on atomically flat surfaces, the topographical influence or the surface roughness can be ignored[8]. Otherwise the cross-talk of the topography, i.e., edge-correlated friction makes it difficult or sometimes even impossible to determine local friction contrasts, which belong to different micromechanical material properties.

In contrast to LFM, the method we use implements a small high-frequency lateral vibrational movement between the tip and sample surface. The amplitude and the phase shift of the harmonically modulated cantilever torsion can be extracted from the photodiode signal using lock-in techniques[9]. Because the lateral vibration is perpendicular to the axis of an I-shaped cantilever, the harmonically modulated friction forces correspond to the twisting of the lever. Force constants for the lever torsion are reported to be very high[10], so nearly all the viscoelastic compression can be related to the polymer surface under investigation.

The first step after the build-up of our harmonically modulated lateral force microscope (HM-LFM) which is based on a commercial apparatus[11], was to compare the sensitivity of LFM and HM-LFM microscopy. Although nearly all friction phenomena in the macroscopic world are based on multi-asperity, investigations of single-asperity interactions should lead to a deeper understanding of elementary frictional processes, i.e., micromechanical properties of polymer surfaces.

## Theoretical aspects

Several models describe the functional dependence of friction as a function of the normal force and are briefly discussed by Meyer et al.[12]. A general approach is the well-known Amonton law, describing the linear relationship between frictional and normal forces with the friction coefficient $\mu$ as a proportional factor. Amonton's law is a consequence of elasto-plastic deformation of many single asperities[13] or, in the case of mainly elastic deformation, of an exponential or Gaussian height distribution of multi-asperities[14] (a multiple tip in contact with a flat surface, a single-asperity tip in contact with a rough surface or a combination of both). The single-asperity interaction can be addressed by using flat and well-defined surfaces and sharp tips as sliding partners and small normal forces. Taking adhesion between tip and surface into account, it was found that the dependence of LFM data from the normal force can be described by the so-called Johnson-Kendall-Roberts (JKR) theory[15]. In some simpler situations, the Hertz model can be used, which is a direct approach to describe the behaviour of solid elastic bodies[16]. The Hertzian model leads to a friction-*vs.*-load$^{2/3}$

relationship; the JKR theory behaves in a similar manner, adhesion forces leading to additional terms[17]. Consequently, only if a friction-*vs.*-load$^{2/3}$ relationship between harmonically modulated friction forces and the normal load can be fitted to measured data with high confidence, a single-asperity geometry should be assumed; otherwise, a multi-asperity interaction between the tip and surface is the appropriate model. From the point of view of micromechanical testing of material properties, the single asperity is better defined and easier to handle in a theoretical framework[18].

## Sample preparation and characterisation

For the purpose of the evaluation of the tip-sample interaction, a flat sample surface with heterogeneous mechanical behaviour (i.e., composition) and with a constant surface roughness and without topography steps at the polymer/polymer interface is needed. Furthermore, the influence of capillary forces[19] present between the tip and the sample, which both are usually covered with a 2-3 nm water film leading to additional attraction, must be avoided. Hence the measurements are performed in distilled water. Additionally, any influence of fluctuations of relative humidity[20] and electrostatic attraction is mostly eliminated by this procedure. In this first approach, diffusion of water into the polymers leading to a decrease in glass transition temperature and thereby to changes in viscoelastic properties is neglected. Because friction forces decrease substantially with increasing humidity during sliding of the tip[21], water acts as a lubricant and reduces the risk of surface damage.

A flat interface between the two immiscible polymers, poly(methyl methacrylate) (PMMA) and polystyrene (PS), was prepared on a freshly cleaved sodium chloride (NaCl) single crystal surface from the melt in a $CO_2$ atmosphere (Fig. 1). The surface roughness of the resulting polymer sample and in particular the topographic step at the PMMA/PS interface can be ignored for most scanning sites.

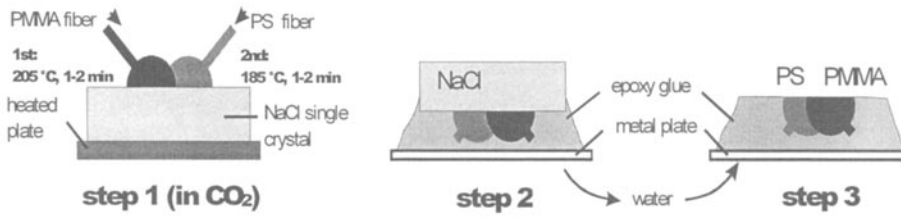


Fig. 1: Preparation of flat polymer/polymer interfaces from the melt. After a PMMA droplet is positioned at 205 °C, the sample is cooled down to 185 °C before adding a PS droplet.

Figure 2 gives a typical optical image of the light reflected by the sample: differences in reflectivity between PS and PMMA facilitate identification of the interface position.

## Experimental

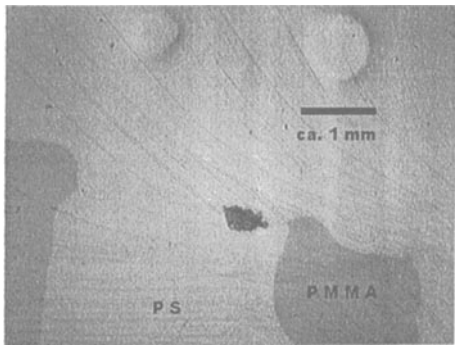


Fig. 2: Optical epimicroscopic image of the sample surface. (The fine lines are a replica of crystallographic multi-steps of NaCl. On the top, two gas bubbles are seen. The dark zone in the middle is a deep hole.)

A sine-wave generator and a synchronized lock-in amplifier are used to apply the piezo voltage and to measure the vibrational torsion amplitude from the photodiode signal, respectively. The resulting amplitude signal is fed into the ADC channel of the SFM (Fig. 3).

I-shaped silicon cantilevers with silicon tips (tip radius 10 nm[22]) are used with a nominal force constant of about 0.2 N/m for the normal direction. The built-in capability of the SFM to measure the force constant via its thermal excitation confirms this value within a range of ±10%. Central element of the HM-LFM is a PZT ceramic piezo plate where a magnetic sample holder is fixed. With an applied voltage of several millivolts at frequencies of 40-100 kHz, a lateral vibration is coupled to the magnet and, consequently, to the sample. Straightforward calculations using the dimensions and electromechanical properties of the piezo show that the lateral movement is in the range of 1.7 nm/mV. However, this value is substantially high because a driven mass of about 6 g is neglected. On the other hand, it is obvious that a superimposed lateral vibration should reduce the lateral sensitivity; however, images with a pixel resolution of about 3 nm were not affected in resolution and sharpness. Hence, it is reasonable to assume that the lateral vibration amplitude is smaller than ≈3 nm.

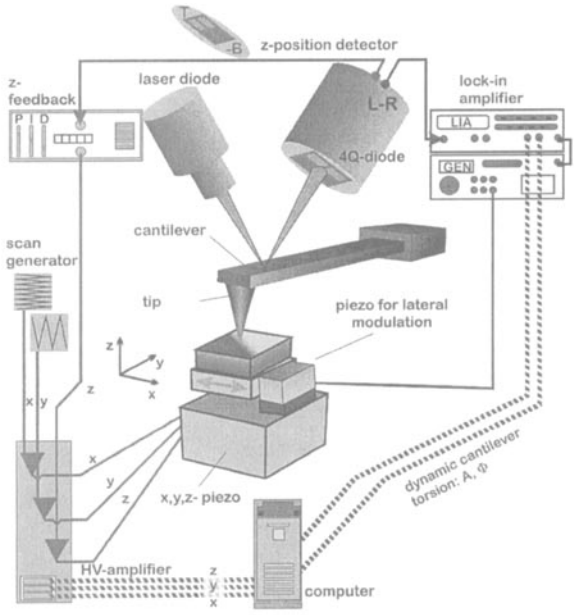


Fig. 3: Scheme of the HM-LFM.

## Results and Discussion

Though the micromechanical interactions between the tip and sample are the main topic of this paper, an additional influence of the scan velocity should be discussed briefly (Fig. 4).

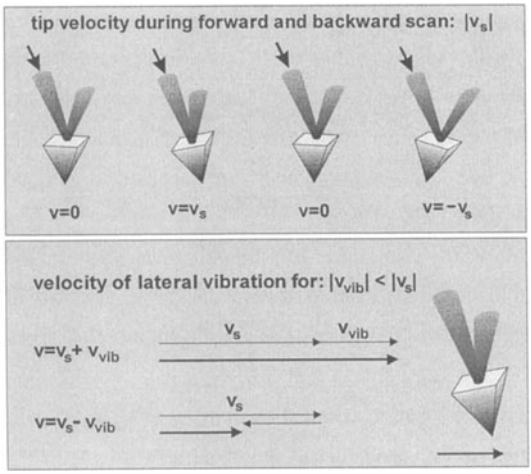


Fig. 4: Relationship between scan velocity and harmonic modulation.

If the vibration velocity in the backward cycle equals the scan velocity, the tip movement is cancelled out for an infinitesimal small period of time. From this critical state down to further decrease in the scan velocity, additional stick-slip behaviour can occur especially for low modulation frequencies. The scan velocity used in Fig. 7 is 40 µm/s and the vibration frequency 44 kHz, which leads to a critical vibration amplitude of 0.91 nm.

Figure 5 shows that an increasing velocity between the tip and surface slightly increases the friction-induced torsion of the SFM cantilever. However, within the same velocity range, the HM-LFM torsion amplitude increases with decreasing scan speed because lower velocities permit the lever to cover a higher angle of torsion.

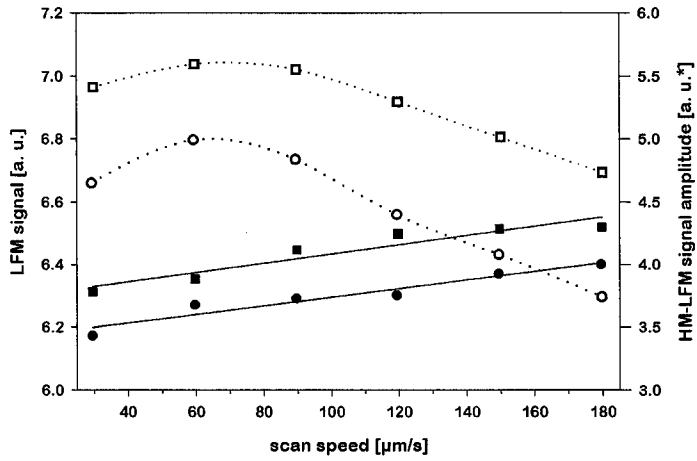


Fig. 5: Scan speed dependence of micromechanical properties of PMMA (□,■) and PS (○, ●) as measured by standard LFM (■, ●) and HM-LFM (□,○). (The lines serve as a guide to the eye.)

Figures 6 a-c give the topography and both the conventional LFM and the HM-LFM information, measured in water to reduce the attractive capillary and electrostatic forces. Because the normal force was as low as possible (≈ 1.5 nN), the LFM image is featureless, although the lever chosen is optimized for LFM and has a high sensitivity to torsional forces (length ≈ 450 μm). But HM-LFM is able to distinguish the difference in micromechanical properties between PS and PMMA quite clearly and with a high signal-to-noise ratio: the upper left-hand (dark) part of Fig. 6c belongs to PS, whereas the lower right-hand (bright) section is PMMA, which can be controlled during the SFM measurements with a built-in optical microscope. This proves that the sensitivity of our HM-LFM measurements of mechanical surface properties is substantially higher than that of the LFM method.

Figure 6a shows that this particular PS/PMMA interface has topographical steps in the order of 20-60 nm and thus edge-induced lever torsion leading to the well-known artefacts in LFM cannot be strictly excluded. All other steps and flat grooves in Fig. 6a are a replica from the NaCl single crystal cleavage steps.

Clearly, the LFM sensitivity can be increased by an increase in the normal force to ≈ 5 nN, as seen in Figs. 7 a-c. Both methods show well correlated contrasts of different micromechanical properties between PS (left-hand side, low LFM and HM-LFM signals, dark) and PMMA (right-hand side, higher LFM and HM-LFM signals, bright). Figure 7a shows that within the image field of Fig. 6, the topographical steps at the interface (1-15 nm) are often in the same range as the average surface roughness (4-6 nm RMS) or even smaller. Such sites are chosen to verify the validity of the different tip - sample interaction models mentioned above and to avoid problems with different frictional behaviour of steps and terraces[12].

Measurements of the dependence of LFM and HM-LFM for the normal load are performed in water at a flat site within the image frame of Fig. 7 with a vibration frequency of 44 kHz and a scan speed of 170 μm/s. The used scan speed is definitely high enough to prevent the stick - slip behaviour (see Fig. 4), the corresponding critical vibration amplitude being 3.9 nm. In every case, the image size was 20x20 μm and the PS/PMMA interface divides the image into two halves. Within these two sections, 10 000 to 20 000 data points (image pixels) are chosen within a rectangular frame and averaged to give one data point of the friction force *vs.* normal force. The images are used without any background correction or other contrast-enhancing image manipulation. Figures 8 a,b show the results.

First of all, it is clear that the sensitivity of detection of micromechanical properties of PS and PMMA using the HM-LFM method is much higher than for LFM microscopy: the material-specific difference in friction force for HM-LFM is very large even for normal forces below 1 nN.

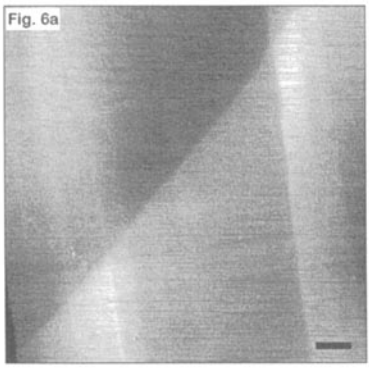


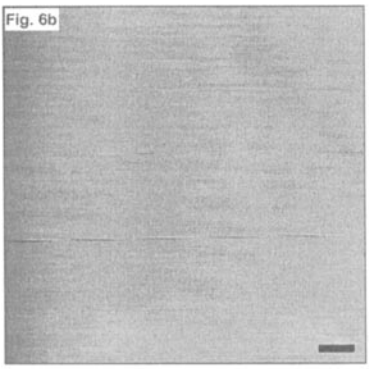


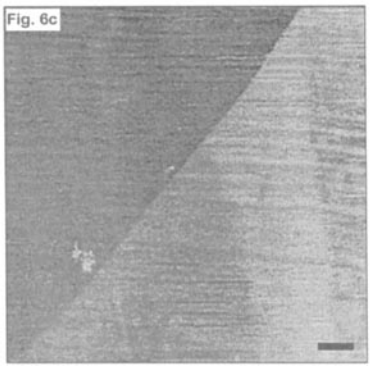


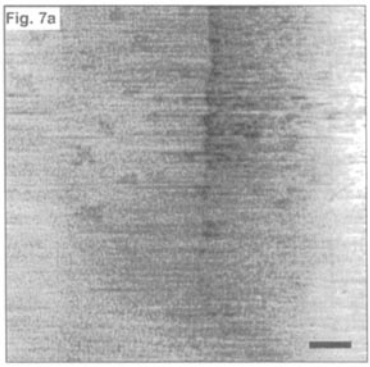


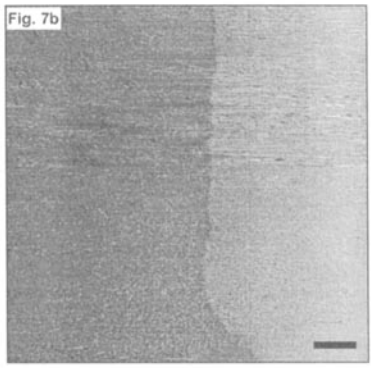


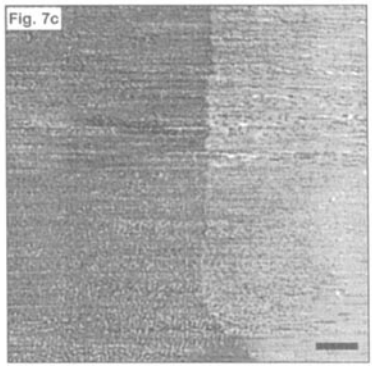


Fig. 6a: Topography at the PS/PMMA interface (image size 150x150 μm, bar 15 μm, Δz range 297 nm, scan speed 150 μm/s, normal load $F_N < 2$ nN, measured in water at 20 °C).
Fig. 6b: Conventional lateral force (LFM) measured simultaneously. (The image is featureless due to the insensitivity of conventional LFM techniques.)
Fig. 6c: Harmonically modulated friction force (HM-LFM) measured simultaneously (lateral vibration < 31 nm, vibration frequency 44 kHz). PS: dark, PMMA: bright.
Fig. 7a: Topography at the PS/PMMA interface (image size 17x17 μm, bar 2 μm, Δz range 57 nm, scan speed 40 μm/s, normal load $F_N \approx 5$ nN, measured in water at 20 °C).
Fig. 7b: LFM measured simultaneously.
Fig. 7c: HM-LFM measured simultaneously (lateral vibration < 31 nm, vibration frequency 44 kHz). PS: dark, PMMA: bright.

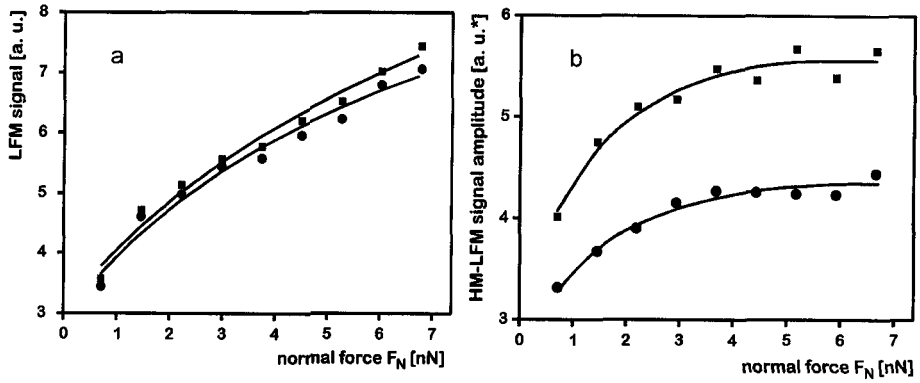


Fig. 8: Lateral force (LFM; a) and harmonically modulated friction force (HM-LFM; b) measured simultaneously (not scaled in the same way) vs. normal force for PMMA (■) and PS (●). Solid line: JKR-fit as a guide to the eye. (Lateral vibration < 31 nm, vibration frequency 44 kHz, scan speed 170 μm/s.)

As already explained in the previous section, the Hertz and JKR models give a relationship between normal and friction force, which can be partially withdrawn by a linear Amonton-like additive term (extended Hertz model or extended JKR model; see Ref.[17], Eqs. 2-4). Although the statistical basis for each point in Fig. 8 is high, some scatter of data is present. This fact and the missing calibration of the torsional force constant of our lever has prevented us so far from extracting exact values for shear strength $t_0$ and pull-off force $F_P$ (i.e., adhesion) by fitting with Eq. 3[17], which is possible if a contact radius of, e.g., 1 nm at $F_N \approx 1$ nN [22,23] is assumed.

Nevertheless, an important observation can be made: obviously, the relationship between frictional and normal forces can be fitted successfully for LFM and HM-LFM measurements on PS and PMMA, respectively. Additionally, the used experimental conditions, the fact that both different polymer surfaces are prepared within one sample at the same topographical level and that both polymers are measured with the same tip and lever and the same laser focus adjustment give a lot of confidence to this interpretation.

A multi-asperity geometry, where either a rough sample surface or a multipoint tip have several contact points linked to each other, leads to an Amonton-like linear relationship between the frictional and normal force. Because our data exclude this, a true single-asperity contact should be considered. This opens a wide field for further investigations because it has not been so far clear that a single-asperity situation could be realised on polymer surfaces. Hence, in the future, we can use calibrated HM-LFM information to determine, e.g., Young's modulus of the sample or the tip-sample geometry even for soft polymer surfaces.

## Conclusion

Harmonically modulated friction force microscopy (HM-LFM) is used to investigate polymer/polymer interfaces. Flat surfaces without edge-depending friction can be prepared, by which it is possible to demonstrate that a single-asperity interaction between the tip and surface takes place. Using the JKR theory, micromechanical properties such as Young's modulus of even very soft samples can be determined with a very low risk of surface damage. It should be noted that the sensitivity of our harmonically modulated lateral force measurements of mechanical surface properties is substantially higher than that of the LFM method, especially for rough surfaces, and less sensitive to artefacts. This high sensitivity could lead to extended and successful application of HM-LFM in the future, especially for soft surfaces, e.g., of polymers and biological materials.

The knowledge of the lateral vibration amplitude is crucial for a deeper understanding of this new technique and should be determined. We will focus on another interesting problem concerning this technique, the dependence of HM-LFM on the scan velocity, especially at low scan speeds.

## Acknowledgements

The author gratefully acknowledges the financial support from the DFG foundation within the research project A1 of the Sfb 605 "Elementary Friction Processes". He also expresses sincere thanks to R. Sernow for technical assistance and Dr. S. Hild (University of Ulm, Experimental Physics), Dr. E. Schulz (BAM, Berlin) and M. Munz (TU Berlin) for valuable suggestions and discussions.

## References

[1] G. Binnig, C. F. Quate, C. Gerber, *Phys. Rev. Lett.* **56**, 930 (1986)

[2] N. A. Burnham, G. Gremaud, A. J. Kulik, P.-J. Gallo, F. Oulevey, *J. Vac. Sci. Technol. B* **14**,1308 (1996); H.-Y. Nie, M. Motomatsu, W. Mizutani, H. Tokumoto, *Thin Solid Films* **273**, 143 (1996); P. Maivald, H. J. Butt, S. A. C. Gould, C. B. Prater, B. Drake, J. A. Gurley, V. B. Elings, P. K. Hansma, *Nanotechnology* **2**, 103 (1991); U. Rabe, M. Dvorak, W. Arnold, *Thin Solid Films* **264**, 165 (1995); M. Motomatsu, H.-J. Nie, W. Mizutani, H. Tokumoto, *Thin Solid Films* **273**, 304 (1996)

[3] A. Hammiche, D.J. Hourston, H. M. Pollock, M. Reading, M. Song, *J. Vac. Sci. Technol. B* **14**, 1486 (1996)

[4] H. Sturm, E. Schulz, *Composites A* **27**, 677 (1996); V. P. Bovtoun, H. Sturm, M. A. Leshchenko, Yu. I. Yakimenko, *Ferroelectrics* **190**, 161 (1997); H. Sturm, W. Stark, V. P. Bovtoun, E. Schulz, *Conf. Proc. 9th Int. Symp. on Electrets (ISE9),* Shanghai 1996, Eds. Z. Xia and H. Zhang, IEEE Service Center, Piscataway NJ (USA), 1996, pp. 223-228; J. T. Dickinson, L. C. Jensen, K. H. Siek, K. W. Hipps, *Rev. Sci. Instr.* **66**, 3803 (1995); M. Yasutake, D. Aoki, M. Fujihira, *Thin Solid Films* **273**, 279 (1996); B. D. Terris, J. E. Stern, D. Rugar, H. J. Mamin, *J. Vac. Sci. Technol. A* **8**, 374 (1990)

[5] J. N. Israelachvilli, Y.-L. Chen, H. Yoshizawa, *Fundamentals of Adhesion and Interfaces*, Eds. D. S. Rimai, L. P. DeMejo and K. L. Mittal, VSP, Utrecht 1995 pp. 261-279

[6] C. M. Mate, G. M. McClelland, R. Erlandsson, S. Chiang, *Phys. Rev. Lett.* **59**, 1942 (1987)

[7] R. Lüthi, E. Meyer, H. Haefke, L. Howald, W. Gutmannsbauer, M. Guggisberg, M. Bammerlin, H.-J. Güntherodt, *Surf. Sci.* **338**, 247 (1995)

[8] M. G. Gee, N. M. Jennet, *Wear* **193**, 133 (1995); J. P. Aimé, Z. Elkaakour, S. Gauthier, D. Michel, T. Bouhacina, J.Curély, *Surf. Sci.* **329**, 149 (1995)

[9] T. Göddenhenrich, S. Müller, C. Heiden. *Rev. Sci. Instrum.* **65**, 2870 (1994); J. Colchero, *Appl. Phys. Lett.* **68**, 2896 (1996)

[10] R. W. Carpick, D. F. Ogletree, M. Salmeron, *Appl. Phys. Lett.*, **70**, 1549 (1997); G. Meyer, N. M. Amer; *Appl. Phys. Lett.* **57**, 2089 (1990)

[11] TOPOMETRIX, Santa Clara, California, 95045-1162 USA

[12] E. Meyer, R. Lüthi, L. Howald, M. Bammerlin, M. Guggisberg, H.-J. Güntherodt, *J. Vac. Sci. Technol. B* **14**, 1285 (1996)

[13] F. P. Bowden, D. Tabor, *The Friction and Lubrication of Solids*, Clarendon, Oxford 1986

[14] J. A. Greenwood, J. B. P. Williamson, *Proc. R. Soc. London, Ser. A* **295**, 300 (1966)

[15] K. L. Johnson, K. Kendall, A. D. Roberts, *Proc. R. Soc. London, Ser. A* **324**, 301 (1971)

[16] C. Putman, R. Kaneko, *Thin Solid Films* **273**, 317 (1996)

[17] The following relationships between frictional and normal forces can be taken from[12]: Amonton's law: $F_F = \mu F_N$ (Eq. 1), with $F_F$, friction force and $F_N$, normal force.
Hertz model: $F_F = \tau_0 \pi [D (F_N - F_P) R]^{2/3}$ (Eq. 2), with $D = \frac{3}{4} [(1-\nu_1^2)/E_1 + (1-\nu_2^2)/E_2]$, $\tau_0$, shear strength, $\nu_i$, Poisson ratio of the tip and sample, $E_i$, Young's moduli of the tip and sample, R, tip (contact) radius and $F_P$, pull-off force.
JKR theory: $F_F = \tau_0 \pi (R/E^*)^{2/3} [(F_N - F_P) + 2F_P + (4F_P (F_N-F_P) + (2 F_P)^2 )^{1/2}]^{2/3}$ (Eq. 3), with $E^* = 3/(4D)$.
From empirical considerations, Eqs. 2 and 3 can be extended by an additive term $\alpha(F_N - F_P)$ (Eq. 4), with $\alpha$, dimensionless material constant similar to $\mu$.

[18] W. Zhong, D. Tománek, *Phys. Rev. Lett.* **64**, 3054 (1990); R. Overney, W. Zhong, D. Tománek. *J. Vac. Sci. Technol. B* **9**, 478 (1991)

[19] R. Kassing, *Scanning Microscopy*, ESPRIT Symp. Proc. DG XIII, Ed. R. Kassing, Springer Verlag, Heidelberg, 1992, pp. 11-31; S. P. Jarvis, T. P. Weihs, A. Oral, J.B. Pethica, *Mater. Res. Soc. Symp. Proc.* **308**, 127 (1993)

[20] A. Schuhmacher, N. Kruse, R. Prins, E. Meyer, R. Lüthi, L. Howald, H.-J. Güntherodt, L. Scandella, *J. Vac. Sci. Technol. B* **14**, 1264 (1996)

[21] M. Bingelli, C. M. Mate, *J. Vac. Sci. Technol B* **13**, 1312 (1995)

[22] Pointprobe lever, $f_{res} \approx 13$ kHz, length $\approx 450$ µm, thickness $\approx 2$ µm, width $\approx 50$ µm, L.O.T. Darmstadt, Germany

[23] M. Heuberger, G. Dietler, L. Schlapbach, *J. Vac. Sci. Technol. B* **14**, 1250 (1996)